Available online at www.sciencedirect.com
SCIENCE DIRECT®
PERGAMON
International Journal of Multiphase Flow 29 (2003) 655–673
International Journal of Multiphase Flow
www.elsevier.com/locate/ijmulflow

# Assessment of turbulent dispersion models for bubbly flows in the low Stokes number limit ☆

F.J. Moraga *,[1], A.E. Larreteguy, D.A. Drew, R.T. Lahey Jr.

*Center for Multiphase Research, Rensselaer Polytechnic Institute, Troy, New York 12180-3590, USA*

Received 7 January 2003; received in revised form 1 February 2003

**Abstract**

Two-fluid turbulent dispersion models have been compared with direct numerical simulations (DNS) of a decaying turbulence bubbly flow in the low Stokes number limit, $St \approx 10^{-3}$. Because of the absence of empiricism, DNS results represent an excellent means of assessing turbulent dispersion models. Sufficiently far away from the inlet of the channel, where the turbulence was fully developed, these turbulent dispersion models were able to predict the DNS results when a Schmidt number, $Sc_b = 0.83$, was used. This result highlights the fact that even bubbles of diameter, $D_b = 42$ μm, considerably smaller than the Kolmogorov length scale, $\eta = 75$ μm, do not behave as passive scalars for which $Sc_b = 1$. In addition, these models were also assessed against a bubbly mixing layer flow having a low Stokes number, $St < 10^{-2}$. Most of the models successfully predicted these mixing layer data. Moreover, for Stokes numbers much smaller than unity several of the models were virtually identical. No adjustable coefficients were used in the mixing layer data comparisons.


*Keywords:* Turbulent dispersion; Two-fluid model; Bubbly flow; Stokes number

## 1. Introduction

Bubbles in a turbulent flow move along fluctuating trajectories as they interact with the turbulent liquid eddies. These fluctuations can disperse the bubbles. Two-fluid models have

☆ This paper was presented in the 4th International Conference on Multiphase Flow (ICMF-2001). The ICMF-2001 took place in New Orleans, USA during the week of May 27 to June 1, 2001 and was attended by 630 delegates representing 46 countries. Professor E.E. Michaelides was the chair of the conference.

* Corresponding author.
*E-mail address:* moragf2@rpi.edu (F.J. Moraga).
[1] Currently at Universidad Argentina de la Empresa, Buenos Aires, Argentina.

0301-9322/03/$ - see front matter 
doi:10.1016/S0301-9322(03)00018-1

accounted for this dispersion by introducing a force proportional to the gradient of the void fraction in the momentum equations of the dispersed phase (Drew and Passman, 1999; Lahey et al., 1993; Carrica et al., 1999; Drew, 2001).

Fully developed vertical duct flow experimental data (Lopez de Bertodano, 1991; Lahey et al., 1993; Alajbegovic et al., 1999), for bubbles or spherical particles of diameter $D \approx 2$ mm, were successfully predicted by assuming that the dispersion force is proportional to the product of the kinetic energy of the liquid phase turbulence and the volume fraction gradient of the dispersed phase.

Similarly, Drew and Passman (1999), Drew (2001) and Lopez de Bertodano (1998) have proposed that the dispersion force is proportional to the Reynolds stress tensor of the dispersed and continuous phase, respectively, and a scalar coefficient, which is a function of the Stokes number (i.e., the ratio of the response times of the bubbles or particles and liquid eddies). Lopez de Bertodano (1998) was able to fit the data of an air/solid-particle jet using this type of model.

Alternatively, Carrica et al. (1999) proposed a model specifically designed for very small bubbles, for which the drag force was dominant. This model has been used for calculating bubbly flows around naval surface ships (Carrica et al., 1999; Larreteguy et al., 1999).

In the model validations carried out by Lopez de Bertodano (1991, 1998), Lahey et al. (1993) and Alajbegovic et al. (1999), there were some sources of uncertainties. In particular, the lift force was modeled and the liquid phase turbulence was characterized by a $k$–$\epsilon$ model, which though widely used, is not free from error.

Druzhinin and Elghobashi (1998) have performed two-phase direct numerical simulations (DNS) of bubbly flows for very small bubbles that obey a Stokes drag law. These simulations provide an excellent test for two-fluid turbulent dispersion models. Not only are there no sources of uncertainties associated with evaluating the dispersion modeling, but the bubbles are exposed to an evolving turbulence field.

In this work the decaying isotropic turbulence DNS of Druzhinin (2000), and the bubbly mixing layer experimental data of Martinez and Lasheras (1997, 2001), were used to assess the turbulent dispersion models discussed above. The methodology employed consisted of using the DNS results to find the optimum turbulent dispersion coefficients for each model and then using the mixing layer data of Martinez and Lasheras (1997, 2001) to evaluate the prediction capabilities of the models in a more complex flow. In addition, analytical comparisons of the models were carried out to show that in the small Stokes number limit they render similar results.

## 2. Description of turbulence dispersion models

Unlike DNS, a two-fluid model predicts the ensemble-averaged bubble velocities and void fraction. [2] Since the instantaneous bubble velocity fluctuations are not resolved, closure laws are necessary to take into account how the fluctuating motion of the liquid disperses the bubbles. The

[2] Notice that both the DNS and the ensemble-average simulations are based on the concept of two interpenetrating fluids. However, the DNS does not require closure laws, while the ensemble-average approach does. Thus we talk about a two-fluid *formulation* and a two-fluid *model* for the DNS and the ensemble-average, respectively.

momentum equation of the bubbles can be derived using ensemble-averaging (Drew and Passman, 1999, Section 11.3; Larreteguy et al., 1999). The result is:

$$\alpha_d \rho_d \left( \frac{\partial \mathbf{u}_d}{\partial t} + \mathbf{u}_d \cdot \nabla \mathbf{u}_d \right) = \nabla \cdot \alpha_d (\mathbf{T}_d + \mathbf{T}_d^{Re}) + \alpha_d \rho_d \mathbf{g} + \mathbf{M}_d - \mathbf{T}_{di} \cdot \nabla \alpha_d, \tag{1}$$

where the subscript d indicates dispersed phase, $\alpha$ is the void fraction, $\rho$ is density, $\mathbf{u}$ is the velocity, $\mathbf{T}_d$, $\mathbf{T}_d^{Re}$ and $\mathbf{T}_{di}$ are the viscous stress tensor, the Reynolds stress tensor, and the interface stress tensor of phase $d$, respectively, and $\mathbf{g}$ is the acceleration of gravity. The interfacial momentum source density, $\mathbf{M}_d$, needs to be constituted in order to achieve closure. In this study drag (D) and turbulent dispersion (TD) dominated the exchange of momentum between the phases. Thus,

$$\mathbf{M}_d \cong \mathbf{M}_d^D + \mathbf{M}_d^{TD}. \tag{2}$$

As in the DNS, Stokes law was used for drag,

$$\mathbf{M}_d^D = -\alpha_d \rho_c \frac{3}{8} \frac{C_D}{R_d} \mathbf{u}_r |\mathbf{u}_r|, \tag{3}$$

where $\mathbf{u}_r$ and $R_d$ are the relative velocity between the bubble and the liquid, and the bubble radius, respectively, and the drag coefficient, $C_D$, for Stokes drag is:

$$C_D = \frac{24}{Re_d} = \frac{12\nu}{|\mathbf{u}_r| R_d}, \tag{4}$$

where $Re_d$ and $\nu$ are the Reynolds number of the bubble and the liquid kinematic viscosity, respectively.

For air bubbles of diameter $D_b = 2R_d = 42$ μm in water moving at their terminal rise velocity, $u_T = D_b^2 g / 18\nu$, it is found that $C_D = 590$. Thus, drag is a dominant force and most other terms in Eq. (1) are negligible, with the exception of buoyancy and turbulence dispersion, $\mathbf{M}_d^{TD}$, which is the main focus of this work. More specifically, we neglect the left-hand side of Eq. (1), the dispersed phase Reynolds stress, and the viscous part of $\mathbf{T}_d$ and $\mathbf{T}_{di}$. It must be noted that the left-hand side of Eq. (1) and the dispersed phase Reynolds stress can be neglected in all flows for which the ratio of discrete and continuous densities is very small, even if the flow of the disperse phase is not dominated by drag. We further assume that the difference between the pressure of phase-$k$, $p_k$, and its interfacial counterpart, $p_{ki}$, $k = c, d$, is negligibly small. This makes it possible to relate the continuous and discrete phase pressures and conclude that for the small bubbles considered in this work, the momentum equation of the discrete phase, Eq. (1), can be approximated as,

$$\mathbf{M}_d^D + \mathbf{M}_d^{TD} + \alpha_d \rho_d \mathbf{g} - \alpha_d \nabla p_c \approx 0. \tag{5}$$

It is worth noting that due to buoyancy the relative bubble velocity is finite. This finite relative velocity, and the large value of the drag coefficient, are what makes drag so dominant in the momentum equation. In addition, the gradient of the continuous phase pressure, $p_c$, cannot be neglected in any analysis that includes gravity, since gravity will produce a hydrostatic pressure gradient. The main purpose of this paper is to study the constitutive models for $\mathbf{M}_d^{TD}$; in particular, The bubble dispersion models which were considered are those of Lopez de Bertodano (1991, 1998), Drew (2001) and Carrica et al. (1999).

### 2.1. The models of Lopez de Bertodano

The following turbulent dispersion model has been widely used:

$$\mathbf{M}_{\mathrm{d}}^{\mathrm{TD}} = -C_{\mathrm{TD}}^{\mathrm{L}} \rho_{\mathrm{c}} k \nabla \alpha_{\mathrm{d}}, \tag{6}$$

where $k$ is the kinetic energy of the turbulence of the continuous phase. This model has been used with a constant (uniform in the computational domain) and variable (non-uniform) values of $C_{\mathrm{TD}}^{L}$. The former version has successfully fit fully developed bubbly and solid/fluid flows in a triangular duct (Lopez de Bertodano, 1991) and a pipe (Alajbegovic et al., 1999; Lahey and Drew, 1999). In both cases the discrete phase consisted of inclusions (bubbles or solid spheres) which were approximately 2 mm in diameter. Thus, the drag coefficient was of the order of unity. A constant coefficient, $C_{\mathrm{TD}}^{L} = 0.1$, fit the data in both cases (Lahey et al., 1993; Alajbegovic et al., 1999).

In an effort to extend the range of applicability of this model, Lopez de Bertodano (1998) proposed a non-uniform turbulent dispersion coefficient for homogeneous turbulence that depends on the Stokes number, $St$, which is the ratio of the time response of the dispersed particles, $\tau_{\mathrm{d}}$, and the liquid eddies, $\tau_{\mathrm{c}}$, respectively. This model was inspired by the work of Reeks (1991), who derived a balance equation for the probability density function (pdf) of the bubbles in phase space. In order to obtain closure, Lopez de Bertodano (1998) assumed that the turbulence autocorrelation function follows the law,

$$\overline{\mathbf{u}_{\mathrm{c}}'(\mathbf{x},0)\mathbf{u}_{\mathrm{c}}'(\mathbf{x},t)} = \overline{\mathbf{u}_{\mathrm{c}}'\mathbf{u}_{\mathrm{c}}'} \exp(-t/\tau_{\mathrm{c}}). \tag{7}$$

With this hypothesis is possible to evaluate analytically the integrals in the work of Reeks (1991), and thus to calculate the dispersion force (Lopez de Bertodano, 1998). The final result for the particular case of isotropic turbulence is the variable coefficient,

$$C_{\mathrm{TD}}^{L} = C_{\mu}^{1/4} \frac{1}{St(1+St)}, \quad St \equiv \tau_{\mathrm{d}}/\tau_{\mathrm{c}}, \tag{8}$$

which coupled with a modified $k$–$\epsilon$ model to account for the extra dissipation introduced by the particles, was successfully used to fit data for a solid/air two-phase jet. In Eq. (8), $C_{\mu}$ is a constant that the $k$–$\epsilon$ model sets to $C_{\mu} = 0.09$, and the bubble response time is given by,

$$\tau_{\mathrm{d}} \equiv \frac{8}{3} \frac{R_{\mathrm{d}}}{C_{\mathrm{D}}|\mathbf{u}_{\mathrm{r}}|}. \tag{9}$$

which, for Stokes law, becomes a constant independent of position, $\tau_{\mathrm{d}} = 2R_{\mathrm{d}}^2/9\nu$.

In order to estimate $\tau_{\mathrm{c}}$ Lopez de Bertodano (1998) considered two contributions. Namely, that of the time scale of the turbulent eddies and that of the time it takes a bubble to move relative to these eddies. The former is,

$$\tau_{\mathrm{c}} = C_{\mu}^{3/4} k/\epsilon, \tag{10}$$

where $\epsilon$ is the dissipation of the turbulence. The latter is the eddy cross over contribution (Loth, 2001; Lopez de Bertodano, 1998), which can be estimated based on the characteristic length scale of the eddies and the relative velocity of the bubble. For the flows considered herein the second contribution was negligible.

It should be noted that Eq. (8) predicts turbulent dispersion coefficients of order unity for bubbles with $St \approx 1$. This prediction is in rough agreement with the experimental findings of Alajbegovic et al. (1999), Lahey et al. (1993), and Lopez de Bertodano (1991) for fully developed conduit flow and 2 mm particles or bubbles. On the other hand, for small bubbles with trajectories dominated by drag, $St \ll 1$, Eq. (8) predicts turbulent dispersion coefficients much larger than unity.

### 2.2. The models of Drew

Drew (Drew and Passman, 1999; Drew, 2001) proposed a turbulent dispersion model for small fluid eddy time scales that is of the form:

$$\mathbf{M}_{\mathrm{d}}^{\mathrm{TD}} = C_{\mathrm{TD}}^{\mathrm{D}} \frac{\rho_{\mathrm{c}}}{\rho_{\mathrm{d}}} \mathbf{T}_{\mathrm{d}}^{Re} \cdot \nabla \alpha_{\mathrm{d}}, \tag{11}$$

where the turbulence dispersion coefficient, $C_{\mathrm{TD}}^{\mathrm{D}}$, is a function of the Stokes number. Lopez de Bertodano (1998) also proposed a model of this form, except that the Reynolds stress of the *continuous* phase takes the place of that of the discrete phase, in the equation above. For isotropic turbulence, the Reynolds stress tensor of the dispersed phase can be written as,

$$\mathbf{T}_{\mathrm{d}}^{Re} = -\tfrac{2}{3}\rho_{\mathrm{d}} k_{\mathrm{d}} \mathbf{I}. \tag{12}$$

In addition, examination of the DNS results that were used in this study show that,

$$k_{\mathrm{c}} \approx k_{\mathrm{d}}. \tag{13}$$

Combining Eqs. (11)–(13), it is concluded that for isotropic turbulence, this model is similar in form to that proposed by Lopez de Bertodano, Eq. (6); however, the values of the coefficient $C_{\mathrm{TD}}^{\mathrm{D}}$ derived by Drew and Passman (1999) were much smaller than those found in the DNS.

Drew (2001) also derived a dispersion model for large eddy times. This model is based on the Boltzmann equation (see Chapman and Cowling, 1939) for the particle probability distribution function $f(\mathbf{x}, \mathbf{u}_{\mathrm{d}}, t)$

$$\frac{\partial f}{\partial t} + \nabla \cdot (\mathbf{u}_{\mathrm{d}} f) + \frac{\partial}{\partial \mathbf{u}_{\mathrm{d}}} \cdot (f \mathbf{a}_{\mathrm{d}}) = 0, \tag{14}$$

where $\mathbf{a}_{\mathrm{d}}$ is the force on an individual particle. Reeks (1991) also started from a kinetic equation, and obtained closure by requiring that the phase space diffusion coefficient be invariant to a random Galilean transformation. Unlike Reeks (1991), Drew put the emphasis on obtaining the dispersion term in the momentum equation and not in the continuity equation. As will be shown below, in the model of Drew (2001), simple physical arguments suffice to obtain closure. Multiplying Eq. (14) by the velocity, and averaging over the fluctuating velocities gives the momentum equation of the discrete phase in the form

$$\frac{\partial n_{\mathrm{d}} \overline{\mathbf{u}}_{\mathrm{d}}}{\partial t} + \nabla \cdot n_{\mathrm{d}} \overline{\mathbf{u}_{\mathrm{d}} \mathbf{u}_{\mathrm{d}}} = \overline{f \mathbf{a}_{\mathrm{d}}} = n_{\mathrm{d}} \mathbf{a}_{\mathrm{d}}(\mathbf{u}_{\mathrm{c}}) + \overline{f \mathbf{a}'_{\mathrm{d}}}. \tag{15}$$

Here $\mathbf{a}_{\mathrm{d}}(\mathbf{u}_{\mathrm{c}})$ denotes the force on the bubble due to the average fluid flow, and $\mathbf{a}'_{\mathrm{d}}$ is the force due to turbulent fluctuations in the fluid. Note that $\overline{f \mathbf{a}'_{\mathrm{d}}}$ is the turbulent dispersion force and $n_{\mathrm{d}}$ is the dispersed phase number density. If we model the probability distribution function as

$$f(\mathbf{x},\mathbf{u}_\mathrm{d},t) \approx n_\mathrm{d}(\zeta) \approx n_\mathrm{d}(\mathbf{x}) + (\zeta - \mathbf{x}) \cdot \nabla n_\mathrm{d}(\mathbf{x}), \tag{16}$$

where $\zeta$ is a position in the neighborhood of $\mathbf{x}$, we see that,

$$\overline{f\mathbf{a}'_\mathrm{d}} \approx \overline{\mathbf{a}'_\mathrm{d}(\zeta - \mathbf{x})} \cdot \nabla n_\mathrm{d}. \tag{17}$$

Thus, in agreement with Reeks (1991), the correlation between force and displacement is the dispersion tensor.

For bubble relaxation times comparable with the eddy time scales, the velocity of the particle will respond to the fluid velocity fluctuations by relaxing to them. However, for eddy times much longer than the bubble relaxation time a particle entrained in an eddy will move in the eddy until it is no longer together. Moreover, we shall assume that the force exerted by the eddies on the particle is constant. Then drag balances the force,

$$\frac{1}{\tau_\mathrm{d}}\mathbf{u}'_\mathrm{d} \approx \mathbf{a}'_\mathrm{d} \tag{18}$$

and the displacement is

$$\zeta - \mathbf{x} \approx \mathbf{u}'_\mathrm{d} t', \tag{19}$$

where $t'$ is time. Hence,

$$\overline{\mathbf{a}'_\mathrm{d}(\boldsymbol{\zeta}\mathbf{x})} \approx \overline{\frac{t'}{\tau_\mathrm{d}}\mathbf{u}'_\mathrm{d}\mathbf{u}'_\mathrm{d}} = -\frac{\tau_\mathrm{e}}{\tau_\mathrm{d}}\overline{\mathbf{u}'_\mathrm{d}\mathbf{u}'_\mathrm{d}},$$

where $\tau_\mathrm{e}$ is the average time that the bubble is entrained in the eddy. If we assume that this time is proportional to the characteristic time of the eddy, we have

$$C^\mathrm{D}_\mathrm{TD} = C^\mathrm{D}_\mathrm{1TD}\frac{\tau_\mathrm{c}}{\tau_\mathrm{d}} = C^\mathrm{D}_\mathrm{1TD}\frac{1}{St}, \tag{20}$$

where $C^\mathrm{D}_\mathrm{1TD}$ is a constant that must be fitted to data.

We note that this model agrees with Lopez de Bertodano (1998), Eq. (8), if the Stokes number, $St$, is much smaller than unity, and $C^\mathrm{D}_\mathrm{1TD} = 3/2C_\mu^{1/4}$.

### 2.3. The model of Carrica

Carrica et al. (1999) proposed,

$$\mathbf{M}^\mathrm{TD}_\mathrm{d} = -C^\mathrm{C}_\mathrm{TD}C_\mathrm{D}\frac{3}{8}\rho_\mathrm{c}\frac{|\mathbf{u}_\mathrm{r}|}{R_\mathrm{d}}\nu^\mathrm{eff}_\mathrm{c}\nabla\alpha_\mathrm{d}, \tag{21}$$

where the turbulent dispersion coefficient $C_\mathrm{TD}$ is defined by:

$$C^\mathrm{C}_\mathrm{TD} = Sc^{-1}_\mathrm{b} = \frac{\nu_\mathrm{bubble}}{\nu^\mathrm{eff}_\mathrm{c}}, \tag{22}$$

and $Sc_\mathrm{b}$ is the Schmidt number of the bubbles, which relates the effective kinematic viscosity, $\nu^\mathrm{eff}_\mathrm{c}$, to the diffusivity of the bubbles, $\nu_\mathrm{bubble}$. Since Eq. (13) indicates that the bubbles in this flow behave approximately as passive scalars, Eq. (22) implies that a coefficient of order unity should fit the data. Note that the eddy viscosity of the $k$–$\epsilon$ model,

$$v_c^T = C_\mu k^2/\epsilon, \tag{23}$$

was used to calculate $v_c^{\text{eff}}$.

The motivation for this model was to obtain a diffusion equation for the void fraction when the momentum equation of the discrete phase is given by Eq. (5). Substituting Eqs. (3) and (21) into Eq. (5) for an assumed hydrostatic pressure gradient yields (Drew and Passman, 1999),

$$(\rho_d - \rho_c)\alpha_d(1-\alpha_d)\mathbf{g} - \alpha_d\rho_c\frac{3}{8}\frac{C_D}{R_d}\mathbf{u}_r|\mathbf{u}_r| - C_{TD}^C C_D\frac{3}{8}\rho_c\frac{|\mathbf{u}_r|}{R_d}v_c^{\text{eff}}\nabla\alpha_d = 0, \tag{24}$$

which, after solving for the relative velocity, $\mathbf{u}_r$, can be written as,

$$\alpha_d\mathbf{u}_r \equiv \alpha_d(\mathbf{u}_d - \mathbf{u}_c) = -C_{TD}^C v_c^{\text{eff}}\nabla\alpha_d + \alpha_d\mathbf{u}_T \equiv -D_d\nabla\alpha_d + \alpha_d\mathbf{u}_T, \tag{25}$$

where $\mathbf{u}_c$ is the velocity of the continuous phase, and $\mathbf{u}_T$ is the terminal rise velocity of the bubbles, given by,

$$\mathbf{u}_T = \frac{8(\rho_d - \rho_c)\alpha_d(1-\alpha_d)R_d\mathbf{g}}{3C_D\rho_c|\mathbf{u}_r|}.$$

The bubble's mass conservation equation,

$$\frac{\partial\alpha_d}{\partial t} + \nabla\cdot\alpha_d\mathbf{u}_d = 0, \tag{26}$$

can rewritten, using Eq. (25), as,

$$\frac{\partial\alpha_d}{\partial t} + \nabla\cdot\alpha_d(\mathbf{u}_c + \mathbf{u}_T) = \nabla\cdot D_d\nabla\alpha_d. \tag{27}$$

This last equation is similar to one which has been frequently used to model diffusive transport in fluids (Taylor, 1953). Thus, the model of Carrica is consistent with modeling the transport of small bubbles by adding a diffusive term to the bubble's mass conservation equation, with the bubble diffusivity given by,

$$D_d = C_{TD}^C v_c^{\text{eff}} = \frac{v_c^{\text{eff}}}{Sc_b}. \tag{28}$$

An important advantage of modeling turbulent dispersion as a force in the momentum equation, rather than as a diffusivity, is that other forces, such as lift and virtual mass, are easily included as additional terms in the momentum equation. This is not the case when dispersion is modeled in the mass conservation equation, as in Eq. (27). The drag coefficient, $C_D$, in Eq. (21) takes into account the expected variation of turbulent dispersion with bubble size. In particular, it provides a simple way to make sure that, for flows dominated by drag, the momentum balance reduces to the form given in Eq. (5). As the bubble size increases, the drag and turbulence dispersion terms in Eq. (1) will become less dominant and other contributions to the momentum of the bubbles will play a more important role.

We will now show that the model of Carrica, the latest model of Lopez de Bertodano (1998) and the model of Drew (2001), given by Eqs. (21), (8)–(10), and (11)–(13), and (20), respectively, are very similar in the passive scalar limit. For this purpose we note that using the expressions given in Eqs. (9), (10), and (23), it is possible to rewrite Eq. (21) as,

$$\mathbf{M}_{\mathrm{d}}^{\mathrm{TD}} = -C_{\mathrm{TD}}^{\mathrm{C}} \rho_{\mathrm{c}} \frac{C_{\mu}^{1/4}}{St} k \nabla \alpha_{\mathrm{d}}. \tag{29}$$

Thus Eq. (6) implies,

$$C_{\mathrm{TD}}^{L} = \frac{C_{\mu}^{1/4}}{St} C_{\mathrm{TD}}^{\mathrm{C}}. \tag{30}$$

This equation clearly shows that for a constant coefficient, $C_{\mathrm{TD}}^{L}$, the models of Lopez de Bertodano (1991) and Carrica et al. (1999) can produce similar results only when the Stokes number varies little in the computational domain. In contrast, for the non-constant coefficient version of the model of Lopez de Bertodano (1998), after combining Eqs. (8) and (30), we find that,

$$C_{\mathrm{TD}}^{\mathrm{C}} = 1/(1 + St).$$

In the passive scalar limit, $St \to 0$, the ratio above tends to unity, and both models should produce very similar results, since $C_{\mathrm{TD}}^{\mathrm{C}}$ is of order unity. We showed in a previous section that the model of Drew (2001) for small Stokes number differs from that of Lopez de Bertodano (1998) by the factor $1/(1 + St)$. Thus, the model of Drew for small Stokes number is identical to that of Carrica et al. (1999) and in this work there was no need to compare the model of Drew and Carrica separately to the DNS simulations.

## 3. Discussion of results of the DNS simulations

DNS of decaying 3D isotropic turbulence was performed for a bubbly flow. A schematic of the two-dimensional flow considered is shown in Fig. 1. The fluid velocity was vertically upwards with a non-dimensional mean advection velocity, $U_0 = 0.6$, and non-dimensional RMS fluid velocity, $u_0 = 0.04$. The inlet and outlet planes were located at $x = 0$ and $x = 4$, respectively.

Bubbles of diameter, $D_{\mathrm{b}} = 42$ μm, obeying a drag Stokes law, were injected at the inlet plane, $x = 0$. At this plane the initial bubble void fraction distribution was Gaussian.

For the sake of simplicity, in all sections of this paper, the ensemble averaging symbol, $\langle\rangle$, is omitted. Unless explicitly stated all quantities are ensemble averaged, as required in two-fluid modeling (Drew and Passman, 1999). The following average quantities were obtained from the DNS simulations:

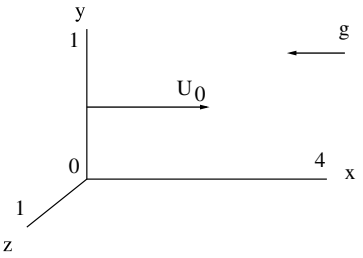


Fig. 1. The geometry of the computational domain in DNS.

- The turbulence kinetic energy of the liquid phase.
- The dissipation of the liquid phase.
- The skewness of the streamwise velocity derivative.
- Void fraction profiles, $\alpha(y)$, at $x = 0, 1, 2$ and 3.5.
- The Reynolds stress of the dispersed phase, $T_{dij}^{Re} = -\langle \alpha \rho_d u'_{di} u'_{dj} \rangle / \langle \alpha \rangle$.

The following power law fits of the turbulence kinetic energy, $k$, and dissipation, $\epsilon$, obtained from the DNS simulations, were used as input for the turbulence dispersion models,

$$k = k_0 \left[ \frac{x - x_s + x_0}{x_0} \right]^{-n}, \qquad \epsilon = \epsilon_0 \left[ \frac{x - x_s + x_0}{x_0} \right]^{-n-1}, \tag{31}$$

where $k_0 = k(x_s)$, $\epsilon_0 = \epsilon(x_s)$ and the DNS data are from the region $x \geqslant x_s = 1$. The fitted parameters were the exponent of the power law, $n$, and the virtual origin, $x_0$. Functions of the form given in Eq. (31) with $1 < n < 1.2$ are known to successfully fit experimental data for single-phase decaying grid turbulence (Hinze, 1987). The analytic solution of the $k$–$\epsilon$ model for homogeneous isotropic decaying turbulence is of the form of Eq. (31), with $n = 1/(C_{\epsilon 2} - 1) = 1.0870$, where $C_{\epsilon 2} = 1.92$ is a constant. Significantly, $n = 1.0870$ successfully fit all DNS results. The virtual origin which results from the fits of the DNS data and the solution predicted by the $k$–$\epsilon$ model can be found in Table 1. Plots of the evolution of the kinetic energy and the dissipation in non-dimensional form can be seen in Fig. 2.

The differences between the DNS and the $k$–$\epsilon$ solutions can be explained by observing that the turbulence Reynolds numbers of the DNS are below the range of applicability of the $k$–$\epsilon$ model. More specifically, for the DNS the Reynolds number based on the turbulence intensity and the integral length scale was 87, while the Reynolds number based on the turbulence intensity and the peak wave number of the initial spectrum was 312. These Reynolds numbers are low compared with grid Reynolds numbers of the experiments ($10^3$) to $10^4$) typically used to calibrate $k$–$\epsilon$ turbulence models (Townsend, 1976).

The skewness of the streamwise velocity derivative grows as $x$ increases until it reaches its asymptotic value at approximately $x = 1$. This skewness is a measure of the average rate of production of enstrophy by vortex stretching, or the rate of nonlinear energy transfer from the low to high wave numbers (Elghobashi and Truesdell, 1992). Thus, until the skewness reaches its asymptotic value at approximately $x = 1$, the predicted turbulence is not valid. For this reason, only the region $x > 1$ was considered for validation of turbulence dispersion models.

Table 1
The virtual origin, $x_0$, for different initial positions, $x_s$

| | $x_s$ | $x_0$ |
|---|---|---|
| DNS fit | 0 | 1.2 |
| $k$–$\epsilon$ solution | 0 | 8.1 |
| DNS fit | 1 | 2.1 |
| $k$–$\epsilon$ solution | 1 | 7.5 |

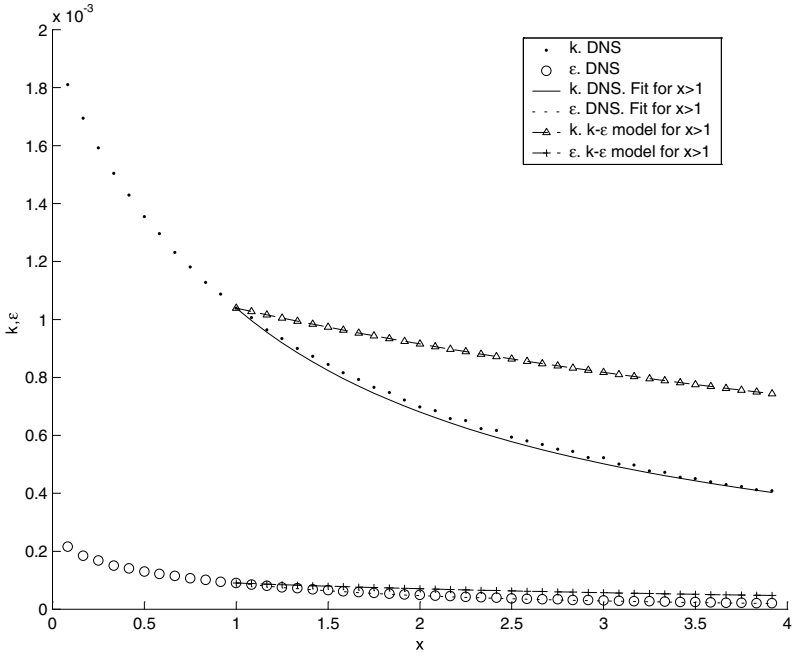


Fig. 2. The kinetic energy and the dissipation in dimensionless form for the DNS simulations and $k$–$\epsilon$ model predictions.

The Stokes number of the DNS data can be estimated using Eqs. (9) and (10) and the plots of the kinetic energy and dissipation of the turbulence in Fig. 2. It is concluded that the Stokes number changes from $St = 1.43 \times 10^{-3}$ at $x = 1$ to $St = 0.91 \times 10^{-3}$ at $x = 4$.

## 4. Two-fluid model predictions of DNS results

The multidimensional computer code CFDShipM (Larreteguy et al., 1999; Carrica et al., 1999) was used to make two-fluid model predictions. In runs 1 and 2 the liquid phase solution came from the DNS results, while in runs 3 and 4 the $k$–$\epsilon$ model was used. This code has been previously used for calculating bubbly flows around naval surface ships (Carrica et al., 1999) and to validate bubbly flow models in simple geometries (Larreteguy et al., 1999, 2002). The inlet boundary condition came from the DNS simulations at $x = 1$. The sides and outlet boundary conditions were,

$$\frac{\partial u_{\mathrm{d}}, v_{\mathrm{d}}, n}{\partial x_i} = 0, \tag{32}$$

where $u_{\mathrm{d}}, v_{\mathrm{d}}, n$ and $x_i$ are the streamwise and lateral bubble velocity, the bubble number density, and the spatial coordinate normal to the boundary surface, respectively. It should be noted that for a monodisperse bubble population the void fraction and the number density are related via the volume of the bubbles. Since from the point of view of the ensemble-averaged flow, the problem is

symmetrical around the $y = 0.5$ axis, only half of the computational domain of the DNS was simulated in the ensemble-averaged runs. In order to diminish the error introduced by the outlet boundary condition, the computational domain was extended to $x = 15 \gg 4$, where $x = 4$ is the end of the computational domain for the DNS simulations. The use of a non-uniform grid made it possible to extend the length of the computational domain without significantly increasing the computational cost. The methodology adopted was to find the optimum turbulent dispersion coefficient that fits the DNS void fraction profile at $x_s + 1$, where $x_s = 1$ was the starting plane of the simulations. The validity of the model was assessed as to how well it fit the remaining void fraction profile.

Table 2 shows a summary of the runs made and their results. Only the constant coefficient version of Lopez de Bertodano (1991) was used. The variation of the Stokes number from $St = 1.43 \times 10^{-3}$ at $x = 1$ to $St = 0.91 \times 10^{-3}$ at $x = 4$, was not considered strong enough to justify the use of the non-uniform version of Lopez de Bertodano (1998). As discussed previously, the region $x < 1$ was excluded from the simulations, since the DNS results there were not fully developed.

As can be seen in Fig. 3, all models fit the DNS predictions quite well. It should be noted that the model of Carrica has a coefficient of order unity. The coefficient $C_{TD}^{C} = 1.2$ in run #2 is a very reasonable value in light of Eq. (22), and the fact that the DNS results indicate that the bubbles behave as passive scalars. The coefficient $C_{TD}^{L} = 500$ obtained for the Lopez de Bertodano (1991) was quite well predicted by Eq. (8), which yields $C_{TD}^{L} \approx 468$, when an average Stokes number of $St = 1.17 \times 10^{-3}$ is used. Thus, the variation of the Stokes number in the computational domain is smooth enough to justify the usage of a constant coefficient, $C_{TD}^{L}$.

It is also interesting to note that putting $C_{TD}^{C} = 1.2$ in Eq. (30), and assuming that the Stokes number changes only due to changes in the bubble diameter (i.e., $\tau_c$ remains constant), indicates that the coefficient $C_{TD}^{L}$ should vary from $C_{TD}^{L} = 500$ for $D_b = 42$ μm to $C_{TD}^{L} \approx 0.1$ for $D_b = 2$ mm, which is consistent with the values found for fully developed conduit flow (Alajbegovic et al., 1999; Lahey et al., 1993; Lahey and Drew, 1999; Lopez de Bertodano, 1991). Thus, it appears that $C_{TD}^{C} = 1.2$ successfully predicts the dispersion behavior of both small and large bubbles.

Runs #3 and 4 were made to study the sensitivity of the turbulent dispersion coefficient to errors in $k$ and $\epsilon$. In Fig. 4 it can be seen that for the models of Lopez de Bertodano and Carrica, the void fraction profiles change very little when the $k$ and $\epsilon$ from the DNS is exchanged by those from the $k$–$\epsilon$ model. This is very interesting, since Fig. 2 indicates significant differences between these predictions. This marked insensitivity to errors in the characterization of the turbulence is apparently due to the fact that if a model overestimates the dispersion coefficient, the result will be

Table 2
Description of two-fluid model simulations made

| Run # | $x_s$ | Dispersion model | $C_{TD}$ for $x_s \leqslant x \leqslant x_s + 1$ | Successful fit for $x > x_s + 1$? | Figure number |
|---|---|---|---|---|---|
| 1 | 1 | Lopez de Bertodano (1991) | 500 | YES | 3(a) |
| 2 | 1 | Carrica | 1.2 | YES | 3(b) |
| 3 | 1 | Carrica and $k$–$\epsilon$ model | 1.2 | YES | 4(a) |
| 4 | 1 | Lopez de Bertodano (1991) and $k$–$\epsilon$ model | 500 | YES | 4(b) |

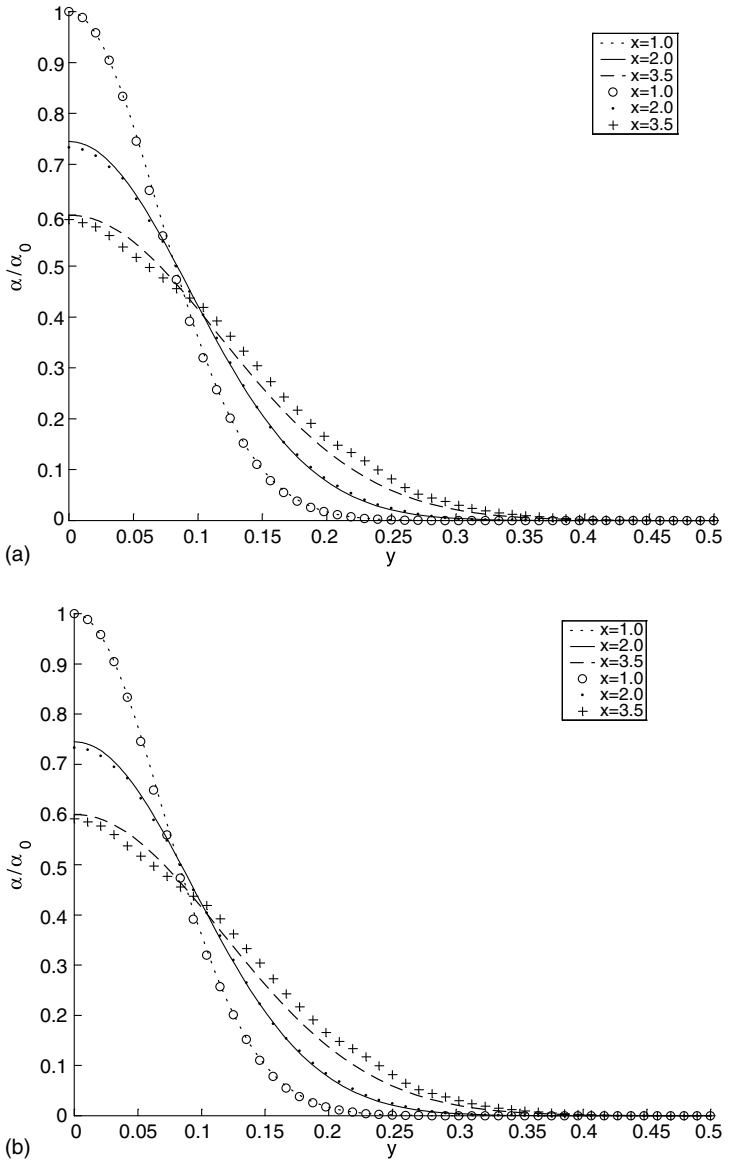


Fig. 3. Void fraction profiles for simulations starting at $x_s = 1$. Symbols: DNS data. Lines: CFDShipM results. (a) Lopez de Bertodano with $C_{TD} = 500$. (b) Carrica et al. with $C_{TD} = 1.2$.

a premature flattening of void fraction gradients, which in turn will reduce bubble dispersion and thus diminish the overestimation. Thus, the error is quickly self-correcting. This insensitivity is highly desirable in most engineering applications, since errors in the turbulent kinetic energy and dissipation may be present. This compensation effect also helps to explain why both models (i.e., that of Carrica et al. (1999) and the constant coefficient version of Lopez de Bertodano (1991)), which model turbulence dispersion very differently, successfully fit the DNS results.

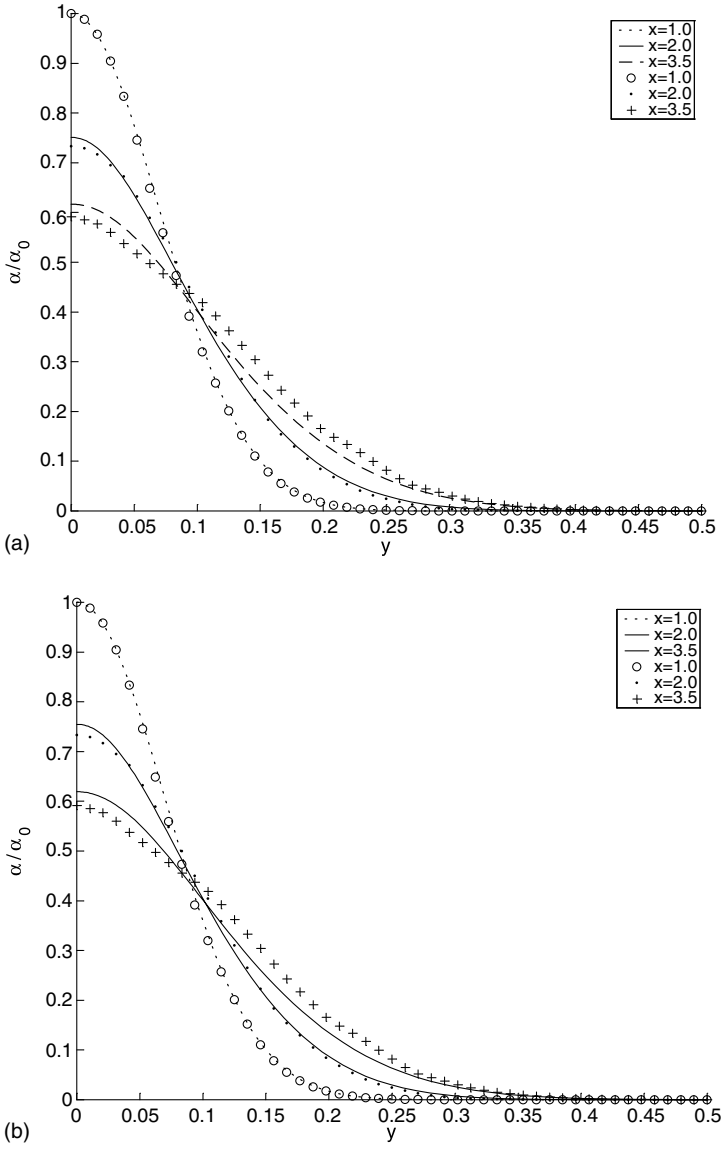


Fig. 4. Void fraction profiles for simulations starting at $x_s = 1$ using $k$–$\epsilon$ model instead of DNS data. Symbols: DNS data. Lines: CFDShipM results. (a) Lopez de Bertodano with $C_{TD} = 500$. (b) Carrica et al. with $C_{TD} = 1.2$.

## 5. The bubbly mixing layer

The results presented previously do not completely assess the prediction capabilities of the models. The DNS simulations were limited to a single bubble size. In addition, isotropic decaying grid turbulence is a relatively simple turbulence structure, and it is desirable to test whether the self-correcting feature of the models will be strong enough to allow the models of Lopez de Bertodano (1991) and Carrica et al. (1999) to yield the same results in a different flow. In the

following sections we will assess the prediction capabilities of the models by simulating the polydisperse bubbly turbulent mixing layer data of Martinez and Lasheras (1997, 2001). This dataset was chosen due to the small Stokes number, $St < 10^{-2}$, quoted by the authors (Martinez and Lasheras, 2001). These simulations were *not* used to obtain a fit for $C_{TD}$, rather the coefficients obtained from the decaying grid turbulence simulations were used. This is particularly appropriate since Martinez and Lasheras (2001) observed that dispersion is independent of bubble size in the range, $St < 10^{-2}$, covered in their data.

### 5.1. Description of the experiment

Martinez and Lasheras (1997) characterized the dispersion of bubbles in a plane, horizontal turbulent mixing layer using a combination of a phase Doppler particle analyzer, and laser scattering measurements. The turbulent shear layer was created by a splitter plate dividing a low velocity stream ($u_1 = 0.07$ m/s) in the upper part from a high velocity stream ($u_2 = 0.28$ m/s) in the lower part. The characteristics of both streams were as follows:

Upper (low velocity) flow:

$$u_1 = 0.07 \text{ m/s},$$
$$u_1^{RMS} = 0.010 \text{ m/s},$$
$$k_1 = 0.0003 \text{ m}^2/\text{s}^2.$$

Lower (high velocity) flow:

$$u_2 = 0.28 \text{ m/s},$$
$$u_2^{RMS} = 0.018 \text{ m/s},$$
$$k_2 = 0.001 \text{ m}^2/\text{s}^2.$$

A uniform concentration of polydisperse size bubbles, with diameters ranging from 10 to 150 μm, was injected in the lower stream of tap water. Many features of the bubbly flow were measured at selected stations (i.e., $x = 0.025$, 0.050, 0.100, 0.150, 0.200, 0.250, 0.300, and 0.350 m) downstream of the trailing edge of the splitter plate. In particular, the bubble's volume probability density function, mean and Sauter mean diameters, and the void fraction profiles in the vertical direction were measured.

## 6. Two-fluid model predictions of a bubbly mixing layer

The computer code CFDShipM (Larreteguy et al., 1999) was again used to carry out two-fluid simulations. Only one-way coupling interactions were considered, since the influence of the bubbles on the liquid was negligible. The domain simulated was [0.025 m−0.600 m] × [−0.140 m−0.190 m], and the edge of the splitter plate corresponds to the location $x = 0$, $y = 0$.

The upstream boundary of the domain has been situated at the position of the first measurement station ($x = 0.025$ m), so as to use the experimental data available there as inlet conditions

for the simulation. The inlet boundary conditions are dominated by the free stream conditions far above and below the splitter-plate, and by the growing turbulent boundary layer close to the plate.

The $k$–$\epsilon$ model was used to model the turbulence of the liquid. Inlet boundary conditions were based on the observation that the free stream kinetic energy of the turbulence, $k$, was about 10–15% of that produced by the shear itself, so it could not be neglected. On the other hand, the boundary layer contribution at the inlet was estimated to be an order of magnitude less than that of the free stream. Thus the splitter plate acted more like a sink than a source of turbulence. The peak of turbulent kinetic energy observed in the experimental results near the plate was then entirely due to production in the shear layer.

The transversal velocity of the carrier phase, $v$, at the inlet was not measured, but could be reasonably estimated from the continuity equation using the experimental measurements of the streamwise liquid velocity, $u$, at the first two measuring stations.

The upper and lower boundaries were considered as slip surfaces, in order to avoid the simulation of the corresponding boundary layers. The downstream boundary conditions were of the form of Eq. (32).

The values of the $C_{\mathrm{TD}}$ coefficients were taken from the previous DNS predictions. Indeed, the idea was to see if the values that were good for a simple flow (decaying homogeneous turbulence), were still good for simulating the more complex mixing layer.

Only drag and turbulent dispersion contributed to the exchange of momentum between the phases. This fact stems from the order of magnitude estimates already presented in the DNS section, and from direct verification by means of numerical simulations, in which the effect of lift was shown to be negligible. Unlike the DNS simulations, the drag law which was used was,

$$C_{\mathrm{D}} = \frac{24}{Re_{\mathrm{d}}}(1 + 0.15Re_{\mathrm{d}}^{0.687}), \tag{33}$$

which quantifies the drag of a dirty-water bubble. We approximated the measured probability density function using four groups of bubble diameters, $D_{\mathrm{b}} = 33$, 52, 66 and 82 μm. These bubbles are small enough to be approximated as rigid spherical bodies when calculating drag coefficients. Since tap water was used in the experiments, there is no need to account for internal circulation as a drag reduction mechanism. Details on the implementation of polydisperse runs into CFDShipM can be found in Carrica et al. (1999).

## 7. Results

Four different options were considered: (1) no turbulent dispersion term, (2) the turbulent dispersion model of Carrica et al. (1999) with $C_{\mathrm{TD}} = 1.2$, (3) the turbulent dispersion model of Lopez de Bertodano (1991) with $C_{\mathrm{TD}}^{L} = 500$, and (4) the turbulent dispersion model of Lopez de Bertodano (1998) with $C_{\mathrm{TD}}^{L} = C_{\mu}^{1/4}/(St(1 + St))$, where the Stokes number was calculated using Eqs. (9) and (10).

In Fig. 5, the experimental void fraction profiles, normalized by the void fraction at the inlet, $\alpha_{\infty}$, are compared against the results obtained for the four above-mentioned models. The width of the upper channel, $L = 0.2$ m, was used as the characteristic length. The results are shown at the locations $x = 0.025$, 0.050, 0.150, and 0.250 m. Fig. 5a shows the fitting of experimental data that

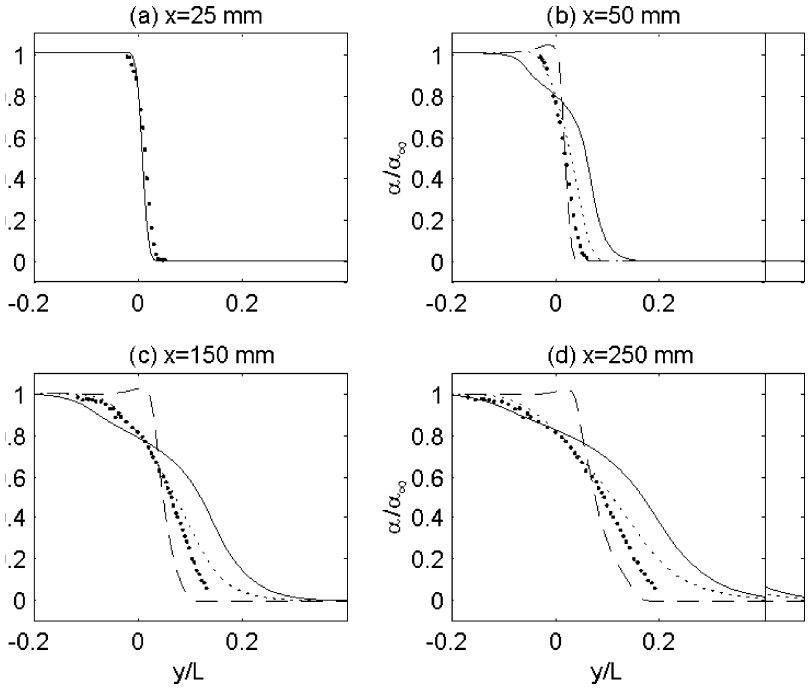


Fig. 5. Dimensionless void fraction profiles at selected measuring stations for polydisperse simulations of a bubbly mixing layer. Symbols: Experimental data. Dashed line: no turbulent dispersion model. Solid line: Lopez de Bertodano (1991) with uniform coefficient, $C_{\mathrm{TD}}^{L} = 500$. Dotted lines: Carrica et al. and Lopez de Bertodano, 1998 with $C_{\mathrm{TD}}^{\mathrm{C}} = 1.2$ and $C_{\mathrm{TD}}^{L} = C_{\mu}^{1/4}/(St(1+St))$, respectively, which are virtually indistinguishable within the resolution of these plots. Figure (a) shows the inlet boundary condition.

was used as the inlet condition for the void fraction. It is clear from the rest of the figures, b, c, and d, that model (1) (*i.e.*, no turbulent dispersion) behaves poorly in the whole domain, which implies that turbulent dispersion plays a key role in this particular problem.

In contrast, the models of Carrica et al. (1999) and Lopez de Bertodano (1998), with a non-uniform coefficient, agree well with the data, but there are some differences between experimental and numerical results in the low void fraction section of the distribution. The same line style, dotted, is used for both models in Fig. 5 because the difference between them is of the order of the the line width. The similarity of the predictions of these two models is not surprising given Eq. (30) and the fact that the Stokes number is much smaller than unity in the whole computational domain and for any bubble size. The very small Stokes number also means that the model of Drew and Carrica are identical for this flow. The differences between the predicted and measured values in the low void fraction region could be attributed to uncertainties on the inlet boundary condition of $k$ and $\epsilon$ and the fact that in this spatially growing flow, small errors at the inlet might amplify downstream. These uncertainties arise from the fact that the $k$ and $\epsilon$ profiles at the inlet were not measured. We believe that given these uncertainties, the agreement between experimental and simulated results of void fraction are excellent for the models of Carrica et al. (1999), Drew (2001) and Lopez de Bertodano (1998). On the other hand, the model of Lopez de Bertodano with a constant coefficient (1991) compares less favorably with the experimental results. Indeed, this

model predicts two different slopes, one in the low velocity region, and a different one in the high velocity region.

The success of the models of Carrica et al., Drew and Lopez de Bertodano may be explained by the fact that the lift and virtual mass forces were negligible, thus leaving us only with turbulent dispersion to compensate for the drag force, which is the situation for which these models were derived. The differences in behaviour between the uniform and non-uniform versions of the Lopez de Bertodano model stems mainly from the differences in the spatial distributions of $k$ and $v_T$ throughout the flow domain. It is also worth mentioning that there was no significant difference between the results of the model of Carrica et al. for the coefficients $C_{TD}^{C} = 1.0$ and 1.2.

Variations in the probability density function of the bubble population, PDF, along the test section, were not measurable (Martinez and Lasheras, 1997). This experimental finding is in agreement with the the prediction by the simulations that turbulent mixing counteracts buoyancy and prevents segregation of the bubbles by size. That is, the PDF predicted when no turbulent dispersion model is used depends strongly on position, while that predicted by the models of Carrica et al. (1999), Drew (2001) and Lopez de Bertodano (1998) is practically independent of position.

## 8. Conclusions

Several turbulent dispersion models have been benchmarked against DNS data for a bubbly flow with $D_b = 42$ μm and Kolmogorov length scale $\eta = 75$ μm. This is the first work that validates turbulent dispersion models in a way that minimizes the modeling uncertainties introduced by factors such as the lift force on the bubbles, or the usage of a turbulence model to characterize the turbulence of the phases.

The model of Carrica et al. (1999), Drew (2001) and Lopez de Bertodano (1998) successfully fit the DNS results in the region $x > 1$ for $C_{TD}^{C} = 1.2$, while that of Lopez de Bertodano (1991) renders a good fit for $C_{TD}^{L} = 500$. In order to assess the prediction capabilities of these models, bubbly mixing layer data were simulated. The models of Carrica, Drew and Lopez de Bertodano, with a non-uniform coefficient, produced the best results. Indeed, these three models produced almost identical results, as was expected from theoretical considerations. In contrast, the constant coefficient version of Lopez de Bertodano (1991) failed to predict the experimental data. This latter model should be used only in flows where the Stokes number is almost constant in the computational domain. It is stressed that these mixing layer simulations are a true assessment of prediction capabilities in the low Stokes number limit, as no coefficient was fitted to the data.

The Schmidt number $Sc_b = 0.83 = 1/C_{TD}^{C} = 1/1.2$ seems a reasonable value when compared to the Schmidt number, $Sc = 0.7$ reported for particle flow in jets and mixing layers (Crowe et al., 1988; Faeth, 1987; Yakhot and Orzag, 1986). A non-trivial result at $Sc_b = 0.83$ was found, which highlights the fact that even bubbles of diameter approximately a half of the Kolmogorov length scale do not behave as passive scalars for which $Sc_b = 1$.

The results presented in this work are strictly valid in the small Stokes number limit. Within this range ($St < 10^{-2}$) Martinez and Lasheras (2001) experimentally observed that dispersion is independent of bubble size, in agreement with our result that the same dispersion coefficients can be used for the mixing layer and the DNS data, spite of differences in the Stokes number. It remains

to explore the behavior of Carrica et al. model for larger bubbles, where $D_b$ is on the order of millimeters and the Stokes number is no longer much smaller than unity. However, experimental data for fully developed pipe flow suggest that Carrica et al.'s model should have a turbulence dispersion coefficient on order of unity even for bubbles as large as $D_b = 2$ mm. The marked insensitivity of the models to errors in the liquid phase turbulence predictions helps explain why $C_{TD}^{C}$ is essentially constant for a wide variety of flows and bubble sizes.

## Acknowledgements

This research was sponsored by the Office of Naval Research under grants N00014-96-10479 (two-fluid modeling) and N00014-96-1-0213 (DNS simulations), respectively.

## References

Alajbegovic, A., Drew, D.A., Lahey Jr., R.T., 1999. An analysis of phase distribution and turbulence structure in disperse particle/liquid flow. Chem. Eng. Comm. 174, 85–133.

Carrica, P.M., Drew, D.A., Lahey Jr., R.T., 1999. A polydisperse model for bubbly two-phase flow around a surface ship. Int. J. Multiphase Flow 25, 257–305.

Chapman, S., Cowling, T.G., 1939. The Mathematical Theory of Non-Uniform Gases. Cambridge University Press.

Crowe, C.T., Chung, J.N., Troutt, T.R., 1988. Particle mixing in free shear flows. Prog. Energy Combust. Sci. 14, 171–194.

Drew, D.A., 2001. A turbulent dispersion model for particles and bubbles. J. Eng. Math. 41, 259–274.

Drew, D.A., Passman, S.L., 1999. Theory of Multicomponent Fluids. Springer.

Druzhinin, O.A., 2000. Description of DNS of a spatially-developing, decaying bubble-laden turbulence. Private communication.

Druzhinin, O.A., Elghobashi, S., 1998. Direct numerical simulations of bubble-laden turbulent flows using the two fluid formulation. Phys. Fluids 10, 685.

Elghobashi, S., Truesdell, G.C., 1992. Direct simulation of particle dispersion in a decaying isotropic turbulence. J. Fluid Mech. 242, 655–700.

Faeth, G.M., 1987. Mixing, transport and combustion in sprays. Prog. Energy Combust. Sci. 13, 293–345.

Hinze, J.O., 1987. Turbulence, second ed. McGraw-Hill.

Lahey, R.T. Jr., Drew, D.A., 1999. An analysis of two-phase flow and heat transfer using a multi-dimensional, multi-field, two-fluid computational fluid dynamics (Cfd) model. Proc. of Japan/US Seminar on Two-Phase Flow Dynamics, UC-SB.

Lahey, R.T.Jr., Bertodano, M., Jones, O.C., 1993. Phase distribution in complex geometry conduits. Nucl. Eng. Des. 141, 177–201.

Larreteguy, A.E., Carrica, P.M., Drew, D.A., Lahey R.T. Jr., 1999. CFDShipM: multiphase code for ship hydrodynamics. Version 2.24 Users manual.

Larreteguy, A.E., Drew, D.A., Lahey R.T. Jr., 2002. A center-averaged two-fluid model for wall-bounded bubbly flows. 2002 Joint US ASME/European Fluids Engineering Division. Summer Meeting, July 14–18, Montreal, Canada.

Lopez de Bertodano, M., 1991. Turbulent bubbly two-phase flow in a triangular duct. Ph.D. Thesis. Rensselaer Polytechnic Institute, Troy, New York.

Lopez de Bertodano, M., 1998. Two fluid model for two-phase turbulent jet. Nucl. Eng. Des. 179, 65–74.

Loth, E., 2001. An Eulerian turbulent diffusion model for particles and bubbles. Int. J. Multiphase Flow 27, 1051–1063.

Martinez, C., Lasheras, J.C., 1997. Dispersion of Bubbles in a Shear Flow. Eleventh International Symposium on Turbulent Shear Flows, Grenoble, France.

Martinez, C., Lasheras, J.C., 2001. Turbulent dispersion of bubbles in a plane shear layer. Exp. Thermal Fluid Sci. 25, 437–445.

Reeks, M.W., 1991. On a kinetic equation for the transport of bubbles in turbulent flows. Phys. Fluids A 3, 446–456.
Taylor, G.I., 1953. Dispersion of soluble matter in solvent flowing slowly through a tube. Proc. Roy. Soc. Lond. A 219, 186.
Townsend, A.A., 1976. The Structure of Turbulent Shear Flows, second ed. Cambridge University Press.
Yakhot, V., Orzag, S.A., 1986. Renormalization group analysis for turbulence. I. Basic Theory. J. Sci. Comput. 1, p. 1.